Journal of Nuclear Materials 389 (2009) 186–190

Contents lists available at ScienceDirect

Journal of Nuclear Materials

journal homepage: www.elsevier.com/locate/jnucmat

Thermophysical properties of several nitrides prepared by spark plasma sintering

H. Muta *, K. Kurosaki, M. Uno, S. Yamanaka

Graduate School of Engineering, Osaka University, Suita, Osaka 565-0871, Japan

A B S T R A C T

Relatively high-density nitride pellets of TiN, ZrN, DyN, UN and their composites have been prepared by spark plasma sintering (SPS) technique without any milling process and sintering additive. The sintering process finished within 30 min for all the samples. The short sintering time and moderate sintering temperature strongly prohibited the grain growth in the sintering process. The SPS-prepared sample showed high Vickers hardness due to the small grain size. Despite of the grain size, the thermal conductivity remains the high value. The result indicates that the impurity layer on particle surface was removed in SPS process. The SPS pelletizing permits easy densification of nitrides without any deterioration of thermal properties, considered to be suitable as a preparation method of nitride fuels.

1. Introduction

The nitride is promising fuel form due to the superior properties such as high thermal conductivity, high melting point, and wide solubility for MA elements with the NaCl type structure. TiN and ZrN are candidates as the diluents for the nitride fuel [1,2]. The TiN or ZrN added composite nitride fuel is expected as a fuel for ADS [3]. However, several problems exist in the fabrication processes. One of the problems is costly-15N extraction [4] and another is the high sintering-resistance of the nitride fuel [5–8]. Conventionally, long milling process, addition of sintering additive, and high sintering temperature were necessary for fabrication of the high-density nitride pellets. The long milling process was not desired because the fabrication processes must be operated remotely. Additionally, the fuel is considered to include some amount of AmN, which easily decomposes and evaporates at high temperature. It means that high temperature and long time heat treatment is not acceptable for the sintering process. Therefore, easy densification method for the nitride pellets has been desired.

Spark plasma sintering (SPS) is a pressure-assisted sintering that utilizes an electric current. The sample temperature was raised and controlled by Joule heating in the sample and electronically conductive dies. The schematic view of the apparatus is shown in Fig. 1. It is known that the sintering temperature and time can be drastically lowered compared with those in conventional sintering [9,10]. High-density pellets of some nitride based ceramics were successfully prepared by the method. The superior feature appears to be suitable for densification of the nitride fuel pellet. In this study, several nitride powders were palletized using the SPS technique. Sample density, the microstructure, and several thermal and mechanical properties were measured and compared with those for samples prepared by conventional sintering way.

2. Experiment

The powders of TiN, ZrN, DyN, UN and their composites were fabricated by carbothermic reduction of carbon-mixed their oxides. Then the pellets were heat treated in a flow of nitrogen–hydrogen mixed gas for removal of the unreacted carbon. The prepared nitride powders were packed to graphite die and sintered in SPS apparatus (SPS-515S, Sumitomo Coal Mining, Japan) in a flow of nitrogen gas. The sintering pressure was 100 MPa for all the samples. The sintering temperature was measured on surface of the graphite die by an optical pyrometer. The temperature program in the sintering process is shown in Fig. 2. Holding time was set to 5 min for all the samples. Consequently, the SPS process, which includes the heating and holding processes, finished within 30 min for all the samples.

The crystal structure and phases were examined by powder X-ray diffraction analysis using Cu Kα radiation. The polished surface of samples was observed by SEM/EDX analysis. The thermal conductivity was evaluated as a product of the thermal diffusivity, the heat capacity, and the experimental density at room temperature. The thermal diffusivity was measured by a laser flash method using TC-7000 equipment (ULVAC Co. Ltd.) in vacuum. Heat capacity was measured using TG-DSC Jupiter (Netzsch Co.) at a flow of argon gas. For DyN and TiN + DyN composite samples, the heat capacity can not be measured because the samples easily oxidized and absorbed water. The Young's modulus was evaluated from the sound velocity measured by ultrasonic pulse echo method using Echometer 1062 (NIHON MATEC Co.). The Vickers hardness was measured by hardness indenter MHT-1 (Matsuzawa Co.) at room temperature.

* Corresponding author.
E-mail address: muta@see.eng.osaka-u.ac.jp (H. Muta).

0022-3115/$ - see front matter © 2009 Elsevier B.V. All rights reserved.
doi:10.1016/j.jnucmat.2009.01.027

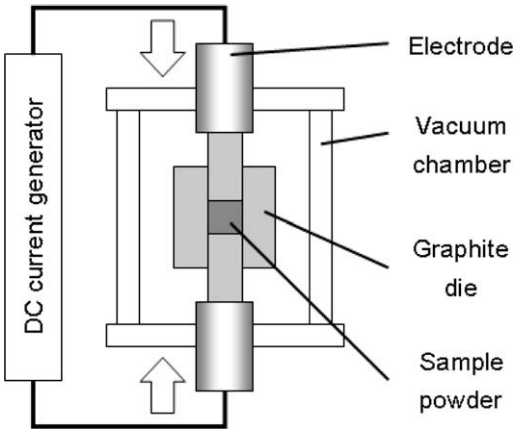

Fig. 1. Schematic view of SPS apparatus.

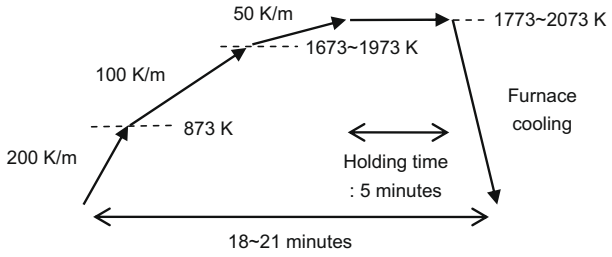

Fig. 2. Temperature program of SPS process.

Table 1
Sample composition, sintering conditions, lattice parameters, and sample density. The sintering time includes heating and holding times.

Sample	SPS temp. (K)	Sintering time (min)	Lattice parameter (nm)	Density (10^3 kg/m^3)	(%T.D.)
TiN	2073	21	0.4243	5.15	95.7
ZrN	2073	21	0.4587	6.45	89.1
UN	1773	18	0.4893	12.9	89.9
TiN + DyN (Ti:Dy = 6:4)	1873	19	TiN:0.4263 DyN:0.4898	6.62	93.8
TiN + UN (Ti:U = 6:4)	1873	19	TiN:0.4263 UN:0.4884	9.4	95.5
$Zr_{0.6}Dy_{0.4}N$	1873	19	0.4721	8.61	102
$Zr_{0.6}U_{0.4}N$	1873	19	0.4699	10.1	96.3

3. Results and discussion

TiN, ZrN, DyN, UN and the four composite pellets were prepared. The sample composition, the lattice parameter and sample density are listed in Table 1 with the sintering conditions. All the nitride pellets were successfully synthesized by the carbothermic reduction and SPS. The XRD patterns for the samples were shown in Fig. 3(a) and (b). The oxides-based impurity peak was small for the samples. The impurity peaks for DyN and TiN + DyN samples were caused by the water absorption in XRD measurement. The peaks corresponding to TiN phase and DyN or UN phase were identified respectively for TiN-added composite pellets. The lattice parameters for TiN, DyN and UN in the composite samples are nearly equal to those for the single phase samples, indicating they were not solved each other. On the other hand, complete solid solution appeared to be formed for ZrN-added samples. It is corresponding to the previous report [11].

Relatively high density (>89%T.D.) pellets were obtained for all the samples. Conventionally such dense nitride pellets were fabricated by sintering at 1873–2273 K for several hours. In this study, the sintering temperature was moderate and the sintering time was drastically short compared to those for the conventional way. It is noted that no sintering additive was added and no milling process had been done for the raw nitride powders. The results indicate that very easy densification for nitride fuel is possible by the SPS technique. It is considered to be caused by the locally-generated high temperature plasma at the particle surfaces. The local high temperature region was generated by concentrated electric current on the limited contact area of particle surface in the SPS process. It activates the particle surface and promoted the neck formation, which resulted in the rapid densification with low sintering temperature. Such characteristics of SPS process is considered to be desirable for the fuel pellet sintering, since the nitride fuel includes some amount of volatile AmN.

Fig. 4 shows SEM images for TiN or ZrN added UN samples together with those for the samples prepared by conventional way. The conventionally-prepared samples were sintered at 2073 K for 8–28 h using 40–65 h ball milled powders [12,13]. The TiN added samples consist of TiN phase (gray colored) and UN phase (white colored), which corresponds to results of XRD patterns. The grain size of each phase is obviously smaller for the SPS-prepared sample. It is caused by the low sintering temperature and short sintering time for the SPS process. It holds true for the ZrN added sample, the SPS prepared $Zr_{0.6}U_{0.4}N$ also possessed significantly small grain size.

Fig. 5 represents temperature dependence of heat capacity for the samples. For comparison, data from SGTE database [14] for

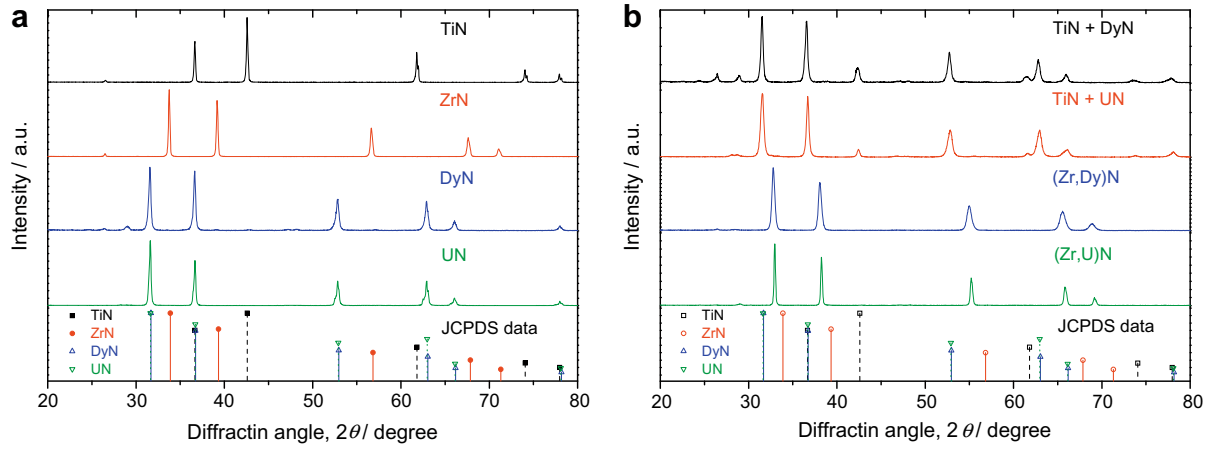

Fig. 3. XRD patterns for SPS-prepared nitride pellets for (a) TiN, ZrN, DyN, UN and (b) their composites.

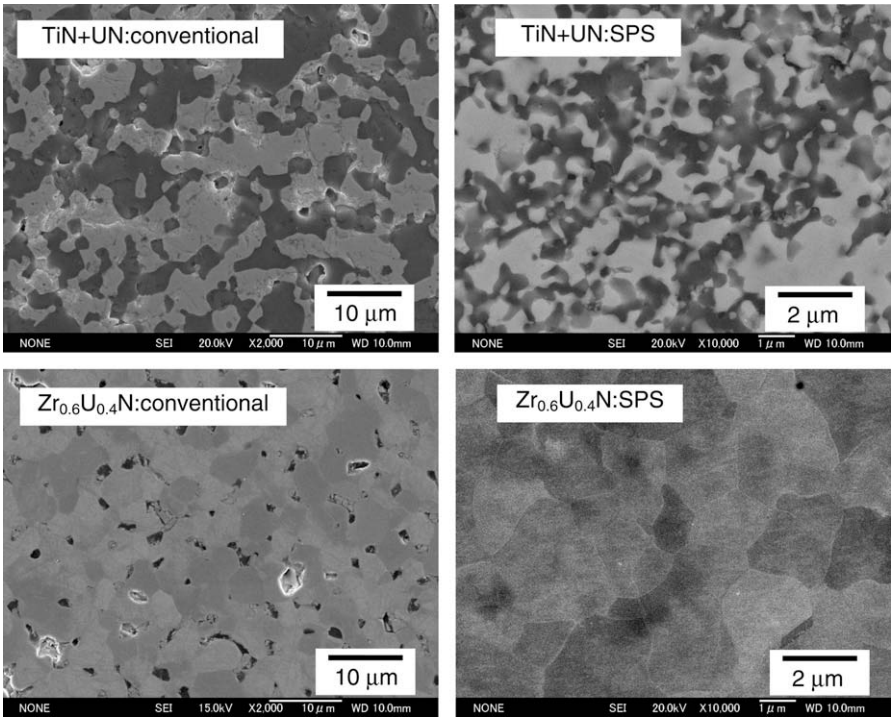

Fig. 4. SEM image of polished surface of TiN + UN and (Zr,U)N prepared by (left) conventional way and (right) SPS.

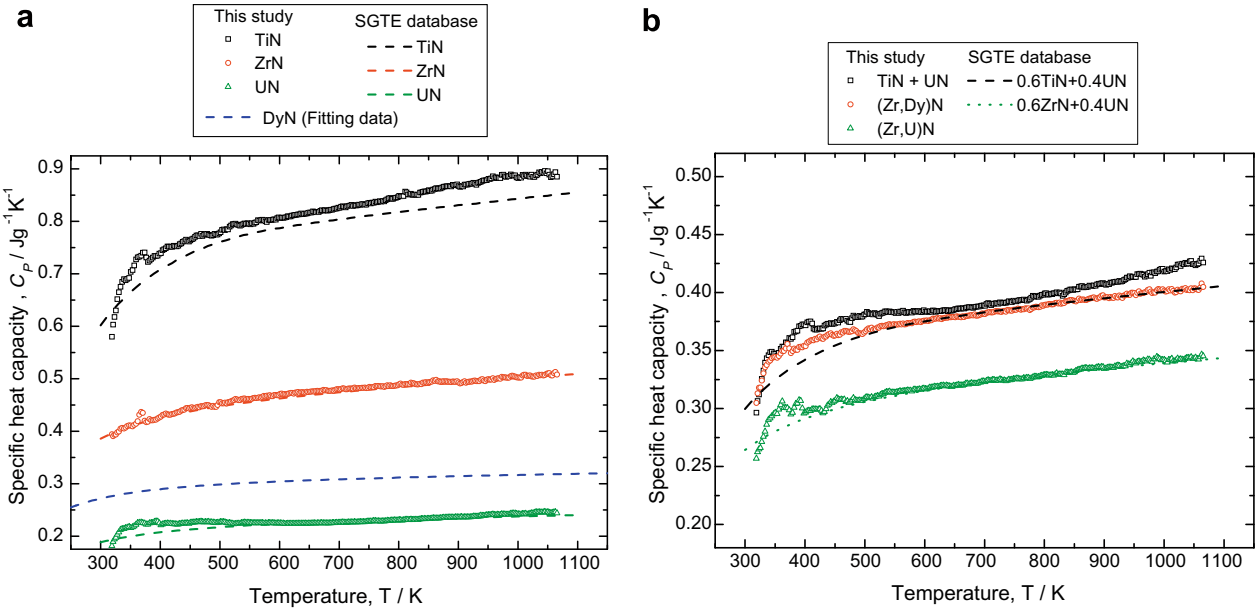

Fig. 5. Temperature dependence of heat capacity for (a) TiN, ZrN, UN and (b) their composites. The curve for DyN is fitting data estimated from heat capacity of ZrN and (Zr,Dy)N.

TiN, ZrN, and UN are shown in Fig. 5(a) together. The heat capacity for our samples is in accordance with the previous data. According to the Neumann–Copp law, the heat capacity for the composite samples is expected to be nearly equal to the sum of their constituent. The calculated value for the composite sample is shown in Fig. 5(b). The data is in good agreement with the experimental values. According to the result, heat capacity for DyN can be estimated from those for ZrN and (Zr,Dy)N sample. The calculated heat capacity for DyN is:

$$C_P(\mathrm{DyN}) = 53.655626 + 0.002790 \times T + 1.19913 \times T^2 - 589942.3313/T^2 \quad (\mathrm{J \cdot mol^{-1} \cdot K^{-1}}).$$

The thermal conductivity for DyN and TiN + DyN composite samples was evaluated using this heat capacity.

The temperature dependence of thermal conductivity is shown in Fig. 6(a) and (b) with previous data [12,15–18]. The values are corrected with consideration of sample density by using following Maxwell–Eucken formula [19]

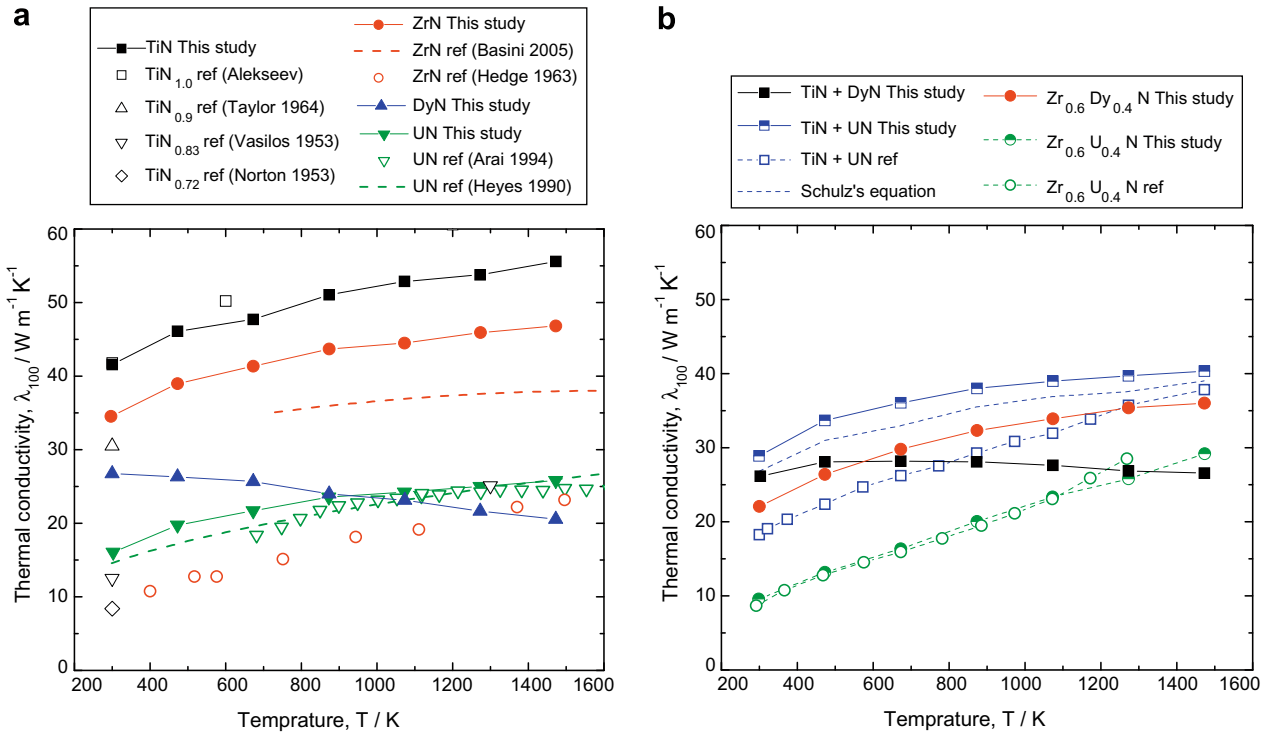

Fig. 6. Temperature dependence of thermal conductivity for (a) TiN, ZrN, DyN, UN and (b) their composites. Lines are guide to eyes.

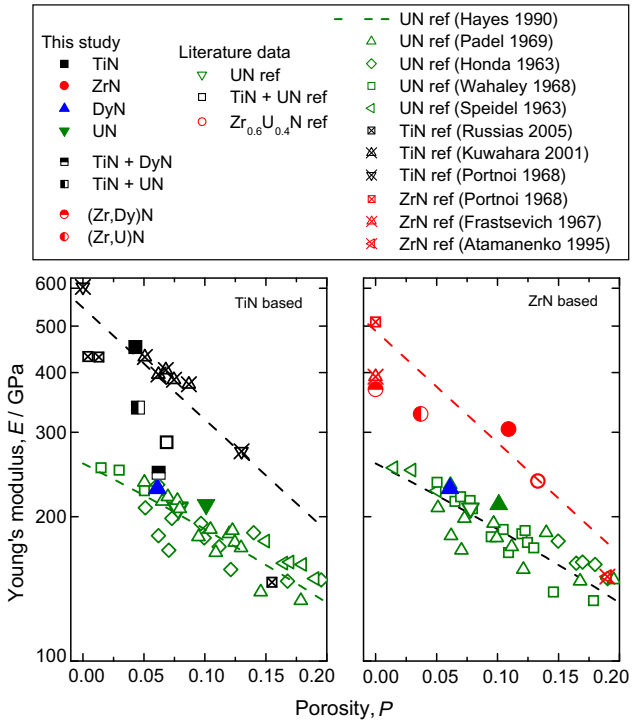

Fig. 7. Porosity dependence of Young's modulus estimated from sound velocity measurement.

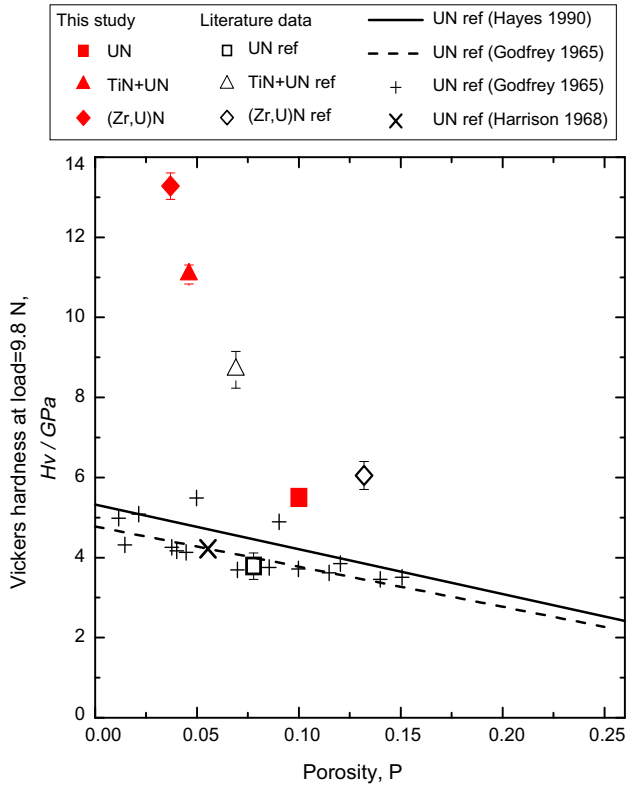

Fig. 8. Porosity dependence of Vickers hardness for UN, TiN + UN and (Zr,U)N.

$$\lambda = \lambda_{100}\frac{1-P}{1+\phi P},$$

where P is volume fraction of pore and λ_{100} is thermal conductivity of sample with the theoretical density. Φ is adjusting parameter that depends on the pore shape. The value of 1.0 is proposed for UN pellet with spherical pores. In this study, same value of 1.0 is used. The thermal conductivity gradually increased with increasing temperature except for DyN and TiN + DyN, which is in agreement with the reported behavior. For DyN, the temperature dependence

should be attributed to the semiconducting behavior, i.e., the electrical conductivity decreased with increasing temperature. The results indicate that the electronic thermal conduction is dominant at the temperature range for the samples. Compared to the previous data, the SPS prepared sample exhibited higher thermal conductivity. It appeared to be strange because their significantly-small grain size generally provides the strong grain boundary scattering for phonons. One possible reason is decrease of the impurity-phonon scattering at the grain boundary. During the sintering process, local high temperature region generated at the particle surface. Hence the thin impurity region on the particle was removed. This 'cleaning' effect supposed to provide the high thermal conductivity. For SPS prepared TiN + UN composite sample, the thermal conductivity takes approximately-same value that is expected by the following Schulz's equation [20] from the data of TiN and UN;

$$1 - C_d = \left(\frac{\lambda_m}{\lambda}\right)^{1/3}\left(\frac{\lambda_d - \lambda}{\lambda_d - \lambda_m}\right),$$

where C_d, λ_m, λ_d, and λ are the volume fraction of precipitate, thermal conductivity of matrix, precipitate, and the composite, respectively. It means that the sample exhibited ideal composite thermal conductivity despite of the sub-micron order grain size as seen in Fig. 4. As a result, the primary high thermal conductivity of the nitride can be remained for the SPS-prepared samples.

For ZrN-added composite sample, (Zr,Dy)N sample shows higher thermal conductivity than (Zr,U)N. It is caused by the strong phonon-impurity scattering for (Zr,U)N. The phonon relaxation time τ_D by the phonon-impurity scattering is expressed by [21,22]:

$$\frac{1}{\tau_D} = A\omega^4,\ A = \frac{\delta^3}{4\pi v^3}\sum_i x_i(1-x_i)\left[\left(\frac{\Delta M}{M}\right)^2 + \left(\frac{\Delta r}{r}\right)^2\right],$$

where ω, δ^3, v are phonon frequency, average atom volume, and sound velocity, respectively. x_i is fractional concentration of the component i. M is atomic mass and r is atomic radius. The mass fluctuation $\Delta M/M$ and strain field fluctuation $\Delta r/r$ determine the scattering degree. Dy and U ion have almost same ionic radius as predicted by the same lattice parameters. Hence the lower thermal conductivity of (Zr,U)N is caused by the larger mass fluctuation between Zr and U atom.

The porosity dependence of Young's modulus is shown in Fig. 7 together with the reported data [12,23–28]. The Young's modulus for the prepared samples is roughly in accordance with the reported value. There was no difference between SPS prepared samples and conventionally-sintered samples. The result indicates the weak grain-size dependence of elastic modulus for the nitrides.

Fig. 8 shows porosity dependence of Vickers hardness for UN, TiN + UN and $Zr_{0.6}U_{0.4}N$ with the previous data [12,29–31]. The filled symbol represents the data for SPS prepared samples. Both TiN and ZrN addition to UN increased the Vickers hardness. Compared to previous data, the sample prepared by SPS showed significantly high Vickers hardness. It is attributed to the very small grain size, which is qualitatively in agreement with Hall–Petch equation.

4. Summary

TiN, ZrN, DyN, UN and their composite powders were prepared by carbothermic method and palletized using SPS technique. The SPS is a pressure-assisted sintering that utilizes Joule heating in the sample. Pellets with 90% of theoretical density were obtained with moderate sintering temperature within 30 min-sintering time, without any milling process and additive. The short sintering strongly restrained the grain growth, which caused the high Vickers hardness for the samples. On the other hand, the Young's modulus was not affected by the difference of sintering way. The samples prepared by SPS showed higher thermal conductivity than those prepared by conventional sintering way despite of the smaller grain size. These results indicate that application of the SPS technique restrains an evaporation of AmN in the sintering process, without deterioration of the thermal properties.

Acknowledgments

The authors deeply appreciate Dr J. Adachi for his assistance of sample observation and provision of his sample data.

Present study is the result of 'Development of advanced nuclear fuels prepared by spark plasma sintering' entrusted to Osaka University by the Ministry of Education, Culture, Sports, Science and Technology of Japan (MEXT).

References

[1] H. Kleykamp, J. Nucl. Mater. 275 (1999) 1.
[2] K. Minato, M. Akabori, M. Takano, Y. Arai, K. Nakajima, A. Itoh, T. Ogawa, J. Nucl. Mater. 320 (2003) 18.
[3] M. Osaka, H. Serizawa, M. Kato, K. Nakajima, Y. Tachi, R. Kitamura, S. Miwa, T. Iwai, K. Tanaka, M. Inoue, Y. Arai, J. Nucl. Sci. Technol. 44 (2007) 309.
[4] Y. Arai, T. Iwai, K. Nakajima, in: Proceedings of International Conference, GLOBAL '97, Yokohama, Japan, 1997, p. 664.
[5] T. Ogawa, J. Nucl. Mater. 201 (1993) 284.
[6] T. Matsui, R.W. Ohse, High Temp. High Press. 19 (1987) 1.
[7] M. Takano, A. Itoh, M. Akabori, J. Nucl. Mater. 294 (2001) 24.
[8] K. Wheeler, P. Peralta, M. Parra, K. McClellan, J. Dunwoody, G. Egeland, J. Nucl. Mater. 366 (2007) 306.
[9] M. Ohyanagi, T. Yamamoto, H. Kitaura, Y. Kodera, T. Ishii, Z.A. Munir, Scr. Mater. 50 (2004) 111.
[10] H.J. Ryu, Y.W. Lee, S. Cha, S.H. Hong, J. Nucl. Mater. 352 (2006) 341.
[11] Y. Arai, K. Nakajima, J. Nucl. Mater. 281 (2000) 244.
[12] J. Adachi, Thermophysical Properties of Advanced Fuels and Higi-burnup Fuels, Doctor Thesis, Osaka University, 2008.
[13] Private communication.
[14] SGTE Pure Substance Database, CHALPAD, 1991.
[15] S.L. Hayes, J.K. Thomas, K.L. Peddicord, J. Nucl. Mater. 171 (1990) 289.
[16] Y. Arai, M. Morihira, T. Ohmichi, J. Nucl. Mater. 202 (1993) 70.
[17] J.C. Hedge, J.W. Kopec, C. Kostenko, J.L. Lang, US At. Energy Comm. ASD-TDR63-597, 1963, p. 128.
[18] V. Basini, J.P. Ottaviani, J.C. Risharud, M. Streit, F. Ingold, J. Nucl. Mater. 344 (2005) 186.
[19] W.D. Kingery, H.K. Howen, D.R. Uhlmann, Introduction to Ceramics, second ed., John Wiley, New York, 1976.
[20] B. Schulz, High Temp. High Press. 13 (1981) 649.
[21] J. Callaway, H.C. von Baeyer, Phys. Rev. 120 (1960) 1149.
[22] B. Abeles, Phys. Rev. 131 (1963) 1906.
[23] A. Padel, C. De Novion, J. Nucl. Mater. 33 (1969) 40.
[24] T. Honda, T. Kikuchi, J. Nucl. Sci. Technol. 6 (1968) 221.
[25] H.L. Whaley, R.A. Potter, W. Fulerson, US At. Energy Comm. Rep. ORNL-4370, 1968, p. 86.
[26] E.O. Speidel, D.L. Keller, US At. Energy Comm. Rep. BMI-1633, 1963, p. 65.
[27] B.A. Atamanenko, Phys. Chem. Mech. Surf. 9 (1995) 281.
[28] K.I. Portnoi, A.A. Mulaseev, V.N. Gribkov, Yu.V. Levinskii, Solvent Powder Metall. Met. Ceram. 8 (1968) 406.
[29] T.G. Godfrey, G. Hallerman, O.B. Cavin, US At. Energy Comm. Rep. ORNL/TM-1050, 1965, p. 142.
[30] T.G. Godfrey, G. Hallerman, US At. Energy Comm. Rep. ORNL-3870, 1965, p. 66.
[31] J.D.L. Harrison, US At. Energy Comm. Rep. ORNL-4330, 1968, p. 28.